Hindawi
Mathematical Problems in Engineering
Volume 2021, Article ID 3797188, 9 pages
https://doi.org/10.1155/2021/3797188

Research Article

Study on Broken Floor Rock Mass by Mining Underground Pressure

Ming Sun, Chen Guo, Wenxiang Zheng, and Huiqiang Duan

Inner Mongolia University of Science and Technology, Baotou, Inner Mongolia 014010, China

Correspondence should be addressed to Ming Sun; sunming831130@126.com

Received 30 April 2021; Revised 28 May 2021; Accepted 19 June 2021; Published 27 June 2021

Academic Editor: Qiuhong Wu

As the dangerous level of floor water inrush in Chinese coal field is becoming more and more serious annually, the widely used formulas of broken floor rock mass are belonged to nonlinear type or empirical type. However, they are not well conformed to the practical situation and including mining underground pressure. The biggest depth of broken floor rock mass and the length of gob-floor or mining-floor until the maximum broken floor location are expressed by theoretical formulas on integrity theory. Taking a mining face in Chinese Anhui Province as the object, the relationship between broken floor rock mass and mining underground pressure is studied by numerical simulation, the theoretical analysis, and the DC exploration. The peak and scope of broken floor rock mass will enlarge until reaching limit value with the increasingly advanced distance. The mining gob stress contour is saddle-shaped, and its growing speed is becoming slower, so the 180 m coal mining face has reached the sufficient mining stage. Wave velocity of broken floor rock mass from 0 m to 16 m is greatly decreased by the mining disturbance, and it is basically conformed to theoretical formula and practical situation. The results can be relatively better used in the pressure mining of the Ordovician limestone, because it can provide some safe guarantee for mining deep coal seam.

1. Introduction

China is the country with the largest coal production and consumption than any other countries in the world. Water inrush from broken floor rock mass is one of difficult problems in Chinese coal field [1–5]. The statistical or the theoretical formulas of broken floor rock mass have made great achievement so far [6–10]. Shi et al. [11, 12] put forward some models using principal component analysis, fuzzy, particle swarm optimization algorithm, and support vector machine. Zhang et al. [13, 14] obtained some formulas by regression analysis fitting and built the model of Fisher's discriminant analysis. Wu et al. [15–19] studied the vulnerable index method based on GIS, ANN, AHP, evidence weight, and logistic regression. Theoretical formulas of broken floor depth were the main consideration of fracture mechanics and plastic mechanics [20]. Relationship between broken floor depth and average mining depth, coal seam dip, mining face height, mining face length, floor resistance ability, and fault fractured zone was analyzed by statistical formula and regression analysis [21, 22]. Theoretical formulas of broken floor depth under stress-damage and flow-damage were derived, and floor damage variable was based on the rock test and floor index [23, 24]. The empirical formula of broken floor depth was analyzed by further error-correction and option-design [25]. Floor aquifuge thickness, weathered zone thickness, grouting section thickness, and broken floor depth were main factors of water inrush coefficient [26]. Weakening effect of acidic solution on the marble is much greater than that on amphibolite [27]. Broken floor depth and safely pressure mining were analyzed from aquifer structure, ecological water level, and water quality [28]. The equivalent Burgers model for revealing the rheological behavior was the combined action of hydraulic pressure and mining stress [29]. Floor rock mass with a fault can tolerate decreases with increasing fault dip and friction angle [30]. The revised shear strength model and experimental data indicated its capability in estimating the peak shear strength of unfilled rock joints [31]. When the inclined work face advanced to about 80 m, the depth of

floor plastic failure zone reached over 15 m [32]. The shear-related roughness classification and strength model of natural rock joint based on fuzzy comprehensive evaluation can be explained objectively [33]. Double criteria for water inrush monitoring and early warning were established based on crack instability extension, water temperature, and water pressure [34]. The PSR model of ecosystem health evaluation and the risk evaluation indicator system were established to scientifically and reasonably assess water inrush risk [35]. Floor water inrush was comprehensively considered from the three aspects of the aquifer's water yield, the hydraulic resistance characteristics of the aquitard, and the tectonic development of the study area [36].

Based on the broken floor rock mass integrity, the biggest depth of broken floor rock mass and the length of gob-floor or mining-floor until the maximum broken floor location are expressed by theoretical formulas. Taking a mining face in Chinese Anhui Province as an object, the relationship between broken floor rock mass and mining underground pressure is studied by numerical simulation, theoretical analysis, and DC exploration. The results will be used well in pressure mining of Ordovician limestone, which can provide some safe guarantee for deep coal mining.

2. Solving Broken Floor Depth and Coal Plastic Scope in Mining-Floor by Integrity

2.1. Solving the Maximum Floor Failure Depth in Mining-Floor by Integrity Theory. According to the slipping line field theory, the broken floor rock mass of mining face is shown in Figure 1, which is caused by advanced abutment pressure and changing underground pressure [37]. In Figure 1, *I* is in token of active stress, *II* is in token of transitional stress, *III* is in token of passive stress, L_1 is the length of broken gob-floor until maximum broken floor location, L_2 is the length of broken mining-floor until maximum broken floor location, x_a is the length of yield zone in unmined coal seam, φ_0 is the interior friction angle, a is the coal mining location, D_m is the maximum broken floor depth, e is the maximum broken floor location, and $a'becd$ is the broken floor mass curve. When the abutment pressure of floor rock mass exceeds its limit value, the plastic deformation and great failure area will appear in broken floor rock mass, and then they can change distribution of underground pressure. Due to the low normal stress and the fixed free surface, the plastic failure area of floor rock mass will move to the back gob by top caving method [38].

The initial broken floor depth in mining-floor rock mass is calculated in formulas (1)–(3), D is the broken floor depth, r_0 is the radius of helix, θ is the angel of ac and ae, φ_0 is the interior friction angle, and α is the angel between ad and ac:

$$D = r_0 \exp(\theta \tan \varphi_0)\sin \alpha, \tag{1}$$

$$r_0 = \frac{x_a}{2\cos((\pi/4) + (\varphi_0/2))}, \tag{2}$$

$$\alpha = \frac{\pi}{2} - \theta + \left(\frac{\pi}{4} - \frac{\phi_0}{2}\right). \tag{3}$$

Taking formulas (2) and (3) into formula (1), the broken floor depth in mining-floor rock mass is calculated in formula (4) by D:

$$D = r_0 \exp(\theta \tan \phi_0)\cos\left(\theta + \frac{\phi_0}{2} - \frac{\pi}{4}\right). \tag{4}$$

When $(dD/d\theta) = 0$, the limit value of formula (4) is the maximum depth of broken floor rock mass by the following formulas:

$$\frac{dD}{d\theta} = r_0 \exp(\theta \tan \phi_0)\cos\left(\theta + \frac{\phi_0}{2} - \frac{\pi}{4}\right)\tan \phi_0 - r_0 \exp(\theta \tan \phi_0)\sin\left(\theta + \frac{\phi_0}{2} - \frac{\pi}{4}\right) = 0, \tag{5}$$

$$\tan \phi_0 = \tan\left(\theta + \frac{\phi_0}{2} - \frac{\pi}{4}\right). \tag{6}$$

The mining-floor integrity is measured by the borehole water quantity. In formula (7), I is the floor rock mass integrity, L_w is the borehole watertight length, and L_t is the borehole total length, and the broken floor rock mass integrity is 7 by I:

$$I = \frac{L_w}{L_t}. \tag{7}$$

Taking formulas (2) and (7) into (4) to the broken floor rock mass integrity, the biggest depth of broken floor rock mass is calculated in formula (8) by D_m:

$$D_m = \frac{L_w x_a \cos \varphi_0}{2L_t \cos((\pi/4) + (\varphi_0/2))}\exp\left[\tan \phi_0\left(\frac{\pi}{4} + \frac{\varphi_0}{2}\right)\right]. \tag{8}$$

Considering broken floor rock mass integrity, the length of broken gob-floor until maximum broken floor location is calculated in formula (9) by L_1 and the length of broken mining-floor until maximum broken floor location is calculated in formula (10) by L_2:

$$L_1 = \frac{L_w x_a \tan \varphi_0((\pi/4) + (\varphi_0/2))\exp((\pi/2)\tan \varphi_0)}{L_t}, \tag{9}$$

$$L_2 = \frac{L_w x_a \sin \varphi_0 \exp[\tan \phi_0((\pi/4) + (\varphi_0/2))]}{2L_t \cos((\pi/4) + (\varphi_0/2))}. \tag{10}$$

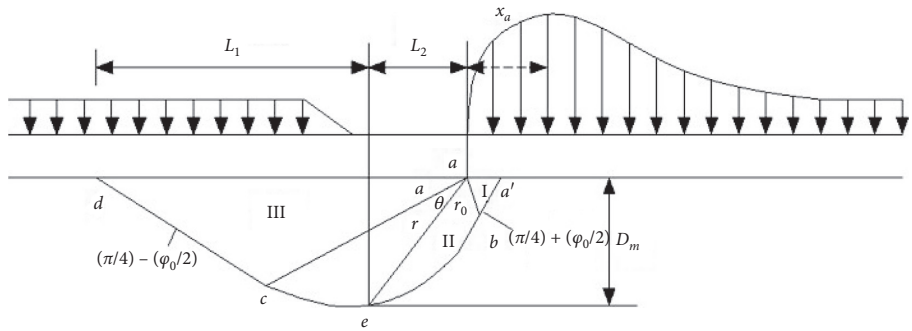

Figure 1: Plastic destroyed area of floor rock mass.

2.2. Solving Coal Plastic Scope in Central Mining-Floor by Integrity. Taking an element of unmined coal seam in equilibrium state, it is dx wide and M high. The zero resultant force along x direction is measured in formulas (11) and (12) [39, 40], where c is the coal cohesive force, σ_x is the overburden weight stress, φ_0 is the interior friction angle, dx is the coal element width, and M is the average mining height:

$$2\left(c+\sigma_x \tan\,\phi_0\right)\mathrm{d}x + M\sigma_x - M\left(\sigma_x + \frac{\mathrm{d}\sigma_x}{\mathrm{d}x}\mathrm{d}x\right) = 0, \quad (11)$$

$$M\frac{\mathrm{d}\sigma_x}{\mathrm{d}x} = 2\left(c+\sigma_x \tan\,\phi_0\right). \quad (12)$$

When differential element reached limit value, considering Mohr–Coulomb strength theory [37], formula (16) is taking formulas (14) and (15) into formula (13), where σ_1 is the coal vertical stress, σ_3 is the coal horizontal stress, σ_z is the coal interfacial stress, and K_1 is the lateral pressure coefficient:

$$\sigma_1 = \frac{1+\sin\,\phi_0}{1-\sin\,\phi_0}\sigma_3 + \frac{2c\cos\,\phi_0}{1-\sin\,\phi_0}, \quad (13)$$

$$\frac{\mathrm{d}\sigma_x}{\mathrm{d}\sigma_z} = \frac{1}{K_1}, \quad (14)$$

$$K_1 = \frac{1+\sin\,\phi_0}{1-\sin\,\phi_0}, \quad (15)$$

$$2\left(c+\sigma_x \tan\,\phi_0\right) - M\frac{\mathrm{d}\sigma_z}{\mathrm{d}x}\frac{1}{K} = 0. \quad (16)$$

Defining the boundary condition ($\sigma_x = 0$ and $x = 0$), formula (16) can be solved and changed formula (17) by σ_z:

$$\sigma_z = cK_1 \cot\,\phi_0 \exp\left(\frac{2K_1 x \tan\,\phi_0}{M}\right) - c\cot\,\phi_0, \quad (17)$$

$$\sigma_z = 10\mathrm{Mr}. \quad (18)$$

Taking formulas (7) and (16) into formula (17), the distance from peak abutment pressure to coal mining face on floor integrity is calculated in formula (18) by x_a, where ϕ_0 is the internal friction angle, c is the coal cohesive force, and M is the average mining height:

$$x_a = \frac{L_w M}{2L_t K_1 \tan\,\varphi_0}\ln\frac{10\mathrm{Mr}+c\,\cot\,\varphi_0}{cK_1\cot\,\varphi_0}. \quad (19)$$

3. Numerical Simulations of Broken Floor Shape and Different Advanced Distance

3.1. Rock Mechanics Parameters of Numerical Simulation. Specific mechanic parameters of broken roof rock, coal seam, and floor rock are given Table 1, which are used in the numerical simulation of the mining face in Chinese Anhui Province.

3.2. Numerical Simulation of Broken Floor Shape and Different Advanced Distance. Due to the limited space, when the coal seam work face advanced to about 180 m, the vertical stress distribution of broken floor rock mass is shown in Figure 2 and the mining failure features of broken floor rock mass are shown in Figure 3. Vertical stress distribution and mining failure features are little changed, but stress concentration in unmined coal seam is much changed, and front abutment pressure peak has reached more than 22 MPa. Stress contour in back gob is saddle-shaped, and its growing speed is becoming slower, so it fully proves that the 180 m coal mining face has been reached sufficient mining stage. With the advancing coal mining face, the limestone shear failure scope in broken floor rock mass is further increasing, but limestone shear failure depth is staying below less than 14 m.

Abutment pressure distribution of floor rock mass and different advanced distance is shown in Figure 4, and the broken depth distribution of floor rock mass and different advanced distance is shown in Figure 5. The abutment pressure coefficient of floor rock mass is changed from 1.2 to 1.6 during the sufficient mining stage, and the peak abutment pressure is varied from 13.5 MPa to 22.7 MPa. Distance between peak abutment pressure and mining face is stayed about 5 m, and the affected length by advanced abutment pressure can reach 20 m. The broken depth of floor rock mass is changed from 8.1 m to 14.2 m, and the maximum was about 15 m. With the advancing working face, the peak and scope of broken floor rock mass will increase until reaching critical value and then basically remain stable.

Table 1: Rock mechanics parameters of numerical simulation.

Lithology	Bulk modulus (GPa)	Shear modulus (GPa)	Unit weight (kg/m^3)	Cohesion power (MPa)	Internal friction angle (°)
Medium sandstone	11.033	8.834	2663.517	26.9	41.8
Siltstone	8.842	6.061	2747.198	18.9	43.4
Mudstone	7.808	6.632	2619.300	12.4	30.8
Coal seam	1.189	1.118	1574.237	12.5	32.0
Mudstone	7.808	6.632	2619.300	12.4	30.8
Siltstone	8.842	6.061	2747.198	18.9	43.4
Fine sandstone	8.798	6.218	2646.739	17.5	42.0
Medium sandstone	11.033	8.834	2663.517	26.9	41.8
Siltstone	8.798	6.218	2664.220	17.5	49.7
Medium sandstone	11.033	8.834	2663.517	26.9	41.8
Mudstone	7.808	6.632	2619.300	12.4	30.8
Fine sandstone	8.798	6.218	2664.220	17.5	49.7
Mudstone	7.808	6.632	2619.300	12.4	30.8

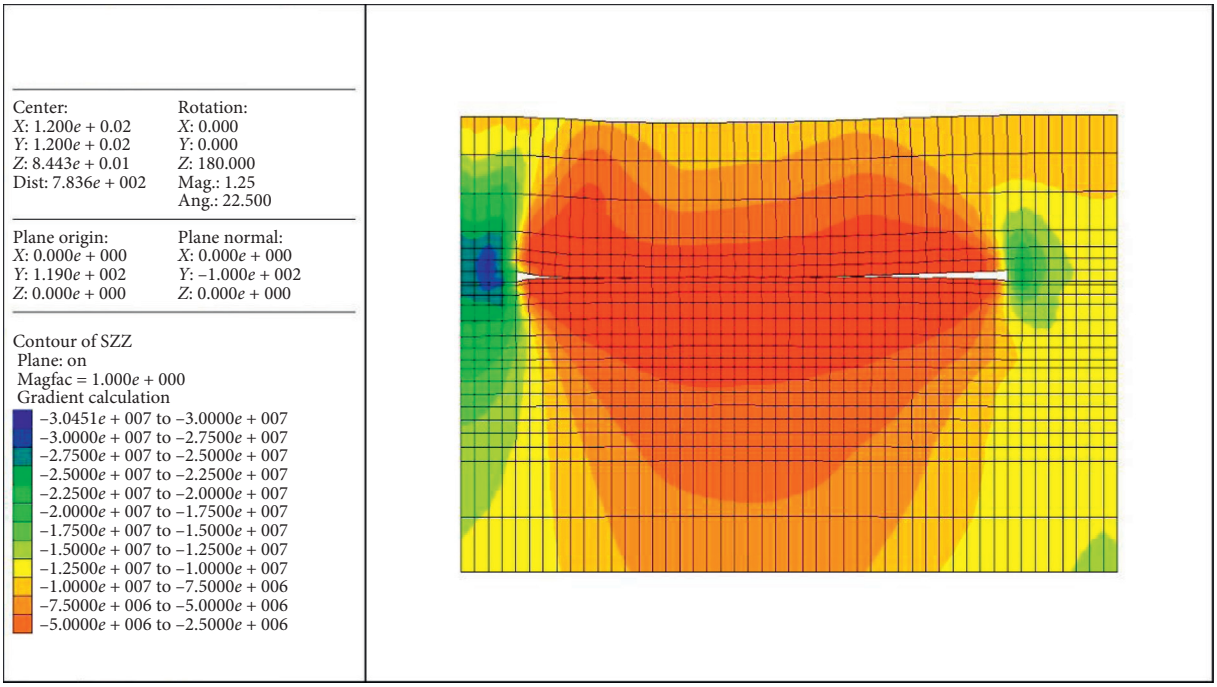

(a)

Figure 2: Continued.

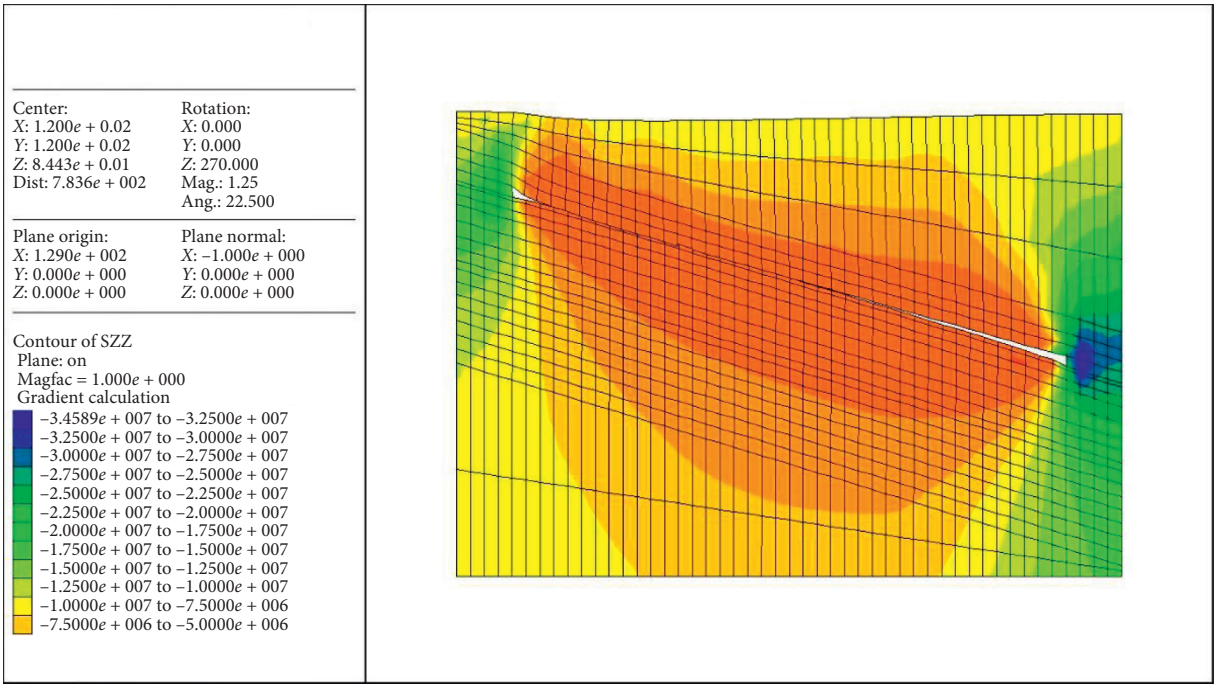

(b)

Figure 2: Vertical stress distribution of broken floor rock mass. (a) Along the advancing direction of coal mining face. (b) Along the inclined direction of coal mining face.

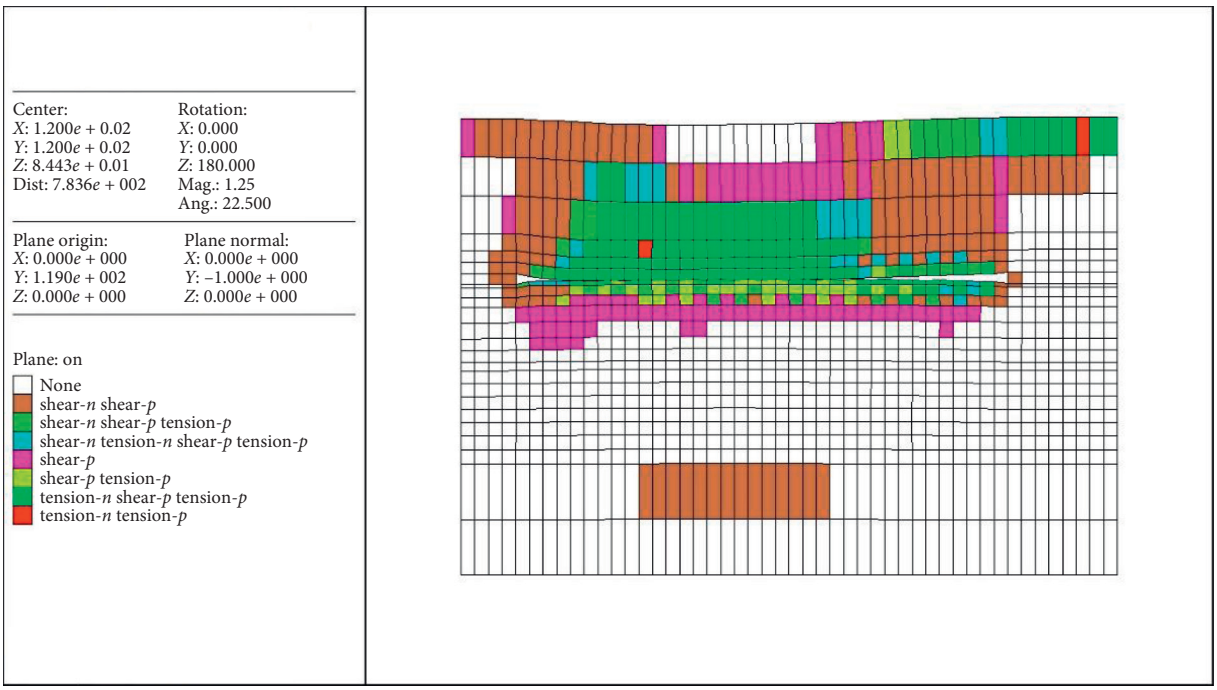

(a)

Figure 3: Continued.

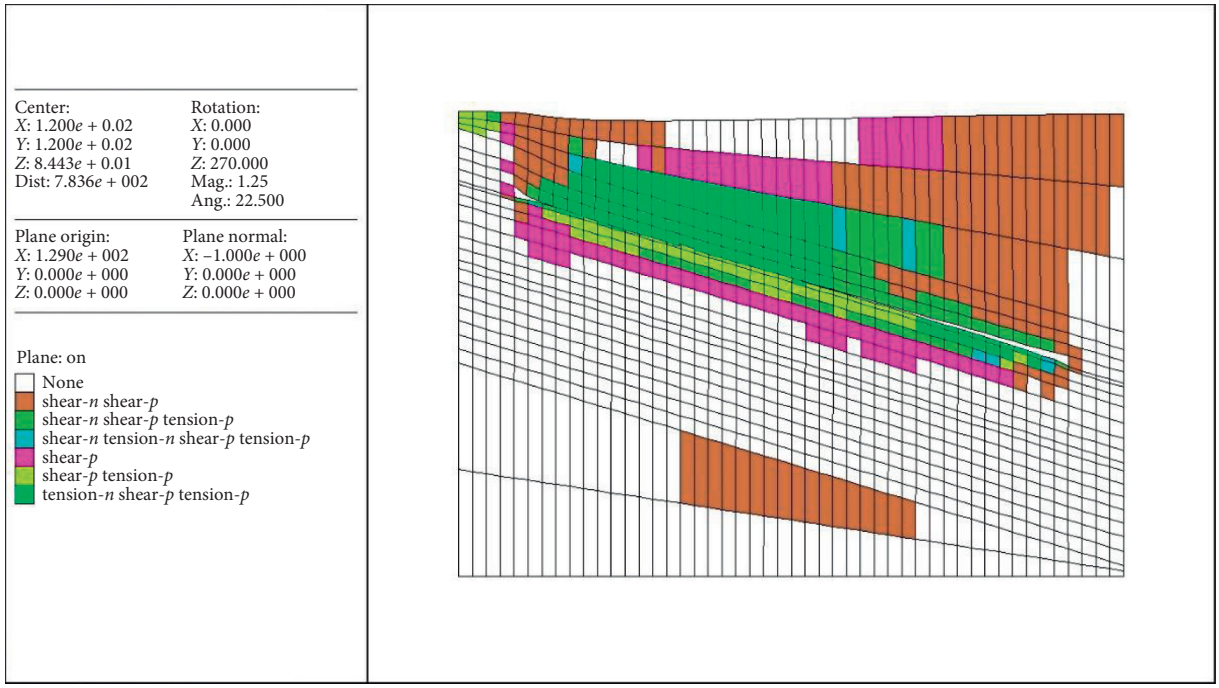

(b)

Figure 3: Mining failure features of broken floor rock mass. (a) Along the advancing direction of coal mining face. (b) Along the inclined direction of coal mining face.

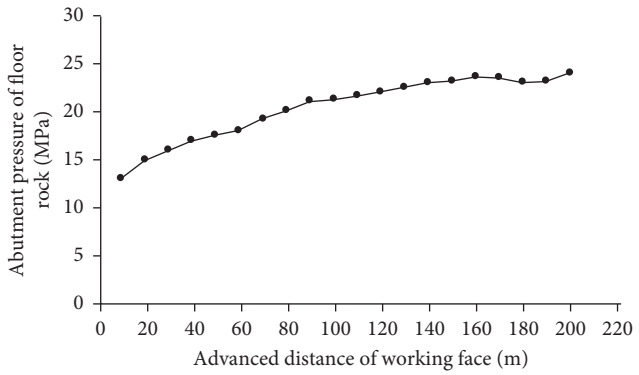

Figure 4: Abutment pressure distribution of floor rock mass.

Figure 5: Broken depth distribution of floor rock mass.

4. Calculating Broken Floor and Observing Wave Velocity of the Mining Face

4.1. Calculating Broken Floor of the Mining Face. Taking a mining face of a colliery in Chinese Anhui Province as the research object, the average buried depth is 466 m, the average mining height is 3.4 m, the stratum bulk density is 2669 kg/m^3, the coal friction angle is 32°, the rock friction angle is 42.6°, static Poisson's ratio is 0.19, the mean cohesive force is 12.5 MPa, and the mining-floor integrity is 0.9.

The biggest depth of broken floor rock mass is as follows by D_m:

$$D_m = \frac{L_w x_a \cos \varphi_0}{2L_t \cos\left((\pi/4) + (\varphi_0/2)\right)} \exp\left[\tan \phi_0 \left(\frac{\pi}{4} + \frac{\varphi_0}{2}\right)\right] = 13.53\,\text{m}. \tag{20}$$

The length of broken gob-floor until maximum broken floor location is as follows by L_1:

$$L_1 = \frac{L_w x_a \tan \varphi_0 \left((\pi/4) + (\varphi_0/2)\right) \exp\left((\pi/2) \tan \varphi_0\right)}{L_t} = 48.76\,\text{m}. \tag{21}$$

The length of broken mining-floor until maximum broken floor location is as follows by L_2:

$$L_2 = \frac{L_w x_a \sin \varphi_0 \exp\left[\tan \phi_0 \left((\pi/4) + (\varphi_0/2)\right)\right]}{2L_t \cos\left((\pi/4) + (\varphi_0/2)\right)} = 12.44\,\text{m}. \tag{22}$$

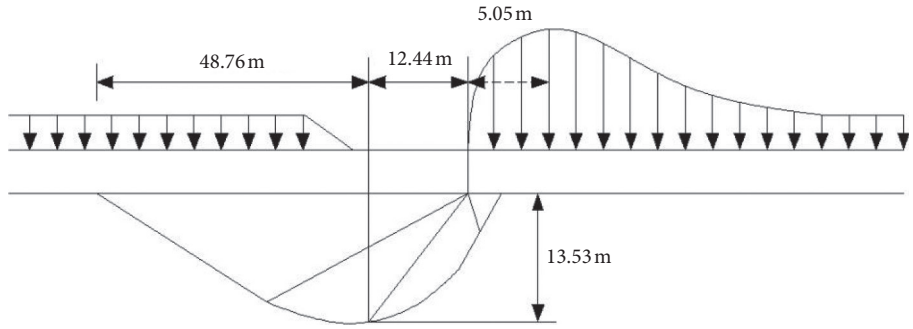

Figure 6: Plastic destroyed area of floor rock mass of a colliery in Chinese Anhui Province.

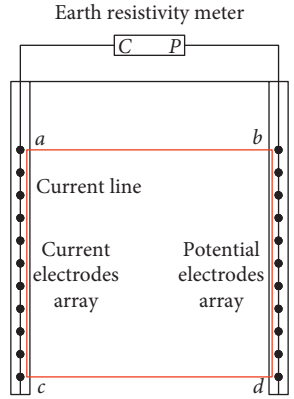

Figure 7: Principle of DC exploration technology.

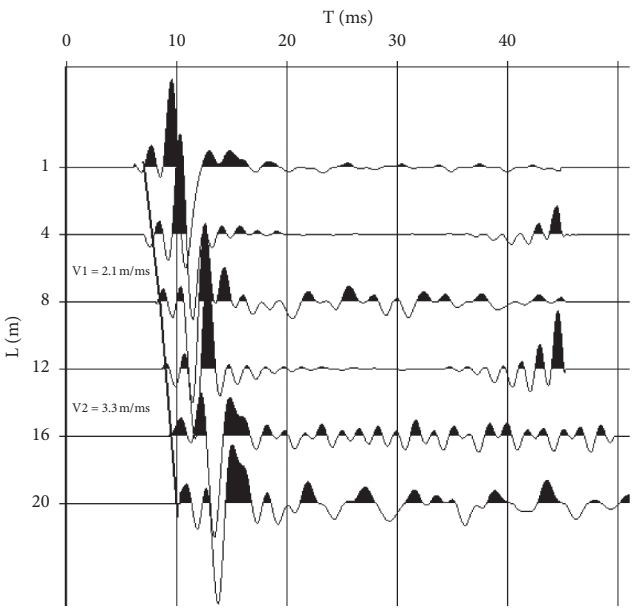

Figure 8: Background wave velocity of borehole.

The distance from peak abutment pressure to coal mining face is as follows by x_a:

$$x_a = \frac{L_w M}{2L_t K_1 \tan \varphi_0} \ln \frac{10\mathrm{Mr} + c \cot \varphi_0}{cK_1 \cot \varphi_0} = 5.05\,\mathrm{m}. \quad (23)$$

Plastic destroyed area of floor rock mass of a colliery in Chinese Anhui Province is drawn in Figure 6.

4.2. Measuring Wave Velocity of Broken Floor Rock Mass by DC Exploration. Figure 7 shows the schematic diagram of DC exploration technology. This method can constantly supply currents into electrodes, repeatedly measure the potential difference, and continuously record different apparent resistivity. So, it can form electric field penetration by *a*, *b*, *c*, and *d* in Figure 7. If floor rock mass is destroyed without water by mining disturbance, the rock conductivity will be weakened, and its resistivity will be gradually increased. If floor rock mass is destroyed with water by mining disturbance, the rock conductivity will be strengthened, and its resistivity will be relatively decreased. If rock resistivity is not obviously changed and basically remains stable, the floor rock mass can be undamaged during coal mining. The floor observed borehole in the ventilation roadway is about 21 m deep, 91 mm diameter, and vertical downward to floor rock mass. Background wave velocity of borehole is shown in Figure 8, and Ming wave velocity of borehole is shown in Figure 9. Floor wave velocity from 0 m to 8 m is 1.7 m/ms, floor wave velocity from 8 m to 16 m is 2.9 m/ms, and floor wave velocity from 16 m to 20 m is 3.2 m/ms. In general, the broken floor rock mass wave velocity from 0 m to 16 m is decreased by coal mining, and it is basically conformed to the calculation results and the actual situations.

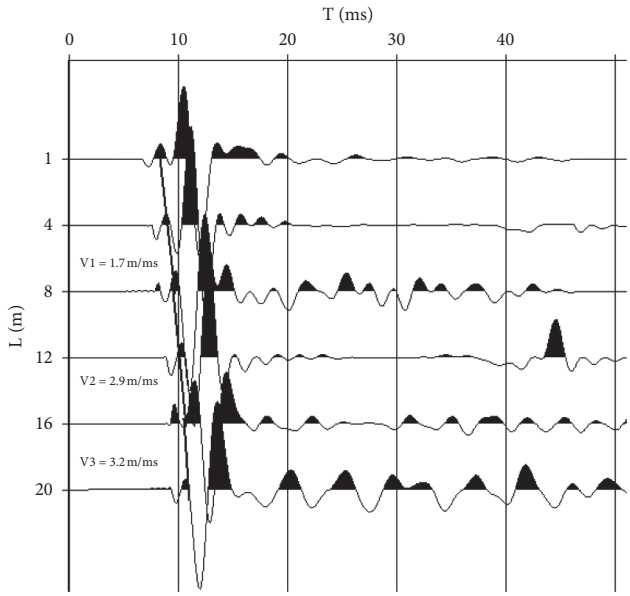

Figure 9: Ming wave velocity of borehole.

5. Conclusions

The biggest depth of broken floor rock mass, length of broken gob-floor or mining-floor until maximum broken floor location, and distance from peak abutment pressure to coal mining face are expressed by theoretical formulas. Stress contour in back gob is saddle-shaped, and its growing speed is becoming slower, so the 180 m mining coal mining face has reached sufficient mining stage. With the advancing coal mining face, limestone shear failure scope in broken floor rock mass is further increasing, but limestone shear failure depth is staying below less than 14 m.

Abutment pressure coefficient of floor rock mass is changed from 1.2 to 1.6 during sufficient mining stage. Because of increasingly advanced distance, the peak and scope of broken floor rack depth will increase until reaching its ultimate limit and then basically remain stable. The biggest depth of broken floor rock mass, length of broken gob-floor and mining-floor until biggest broken floor location, and distance from peak abutment pressure to coal mining face are calculated by a colliery in Chinese Anhui Province. Floor rock mass wave velocity from 0 m to 8 m and from 8 m to 16 m is 1.7 m/ms and 2.9 m/ms by DC, so floor rock from 0 m to 16 m is greatly changed by mining disturbance and basically conformed to theoretical calculation.

These calculation results are well consistent with the actual situation, which shows that the used models are feasible and reasonable. Dynamic evolution and disaster mechanism of broken floor rock mass and the increasingly mining advanced distance by underground pressure will be studied by water pressure and tectonic stress for future research direction. Locating the weak link of waterproof layers in broken floor rock mass and identifying the source of water hazards accurately are the key step in water inrush prevention and control.

Data Availability

The data used to support the findings of this study are included within the article.

Conflicts of Interest

The authors declare that there are no conflicts of interest regarding the publication of this paper.

Acknowledgments

This study was supported by the Inner Mongolia Autonomous Region Natural Science Foundation (2019MS05042 and 2019MS05053).

References

[1] L. Q. Shi, R. G. Zhang, D. J. Xu, Y. Li, M. Qiu, and W. F. Gao, "Prediction of water inrush from floor based on GWO-Elman neural network," *Journal of China Coal Society*, vol. 45, no. 7, pp. 2455–2463, 2020.

[2] W. P. Li, W. Qiao, X. Q. Li, and R. H. Sun, "Characteristics of water disaster, evaluation methods and exploration direction for controlling groundwater in deep mining," *Journal of China Coal Society*, vol. 44, no. 8, pp. 2437–2448, 2019.

[3] X. G. Yu, J. Han, L. Q. Shi, Y. Wang, and Y. P. Zhao, "Application of a BP neural network in predicting destroyed floor depth caused by underground pressure," *Environment Earth Science*, vol. 76, no. 76, p. 12, 2017.

[4] Q. B. Zhao, X. N. Zhao, Q. Zhao, C. W. Liu, and X. L. Wang, "Water burst mechanism of 'divided period and section burst' at deep coal seam floor in North China type coalfield mining area," *Journal of China Coal Society*, vol. 40, no. 7, pp. 1601–1607, 2015.

[5] Q. Wu, X. Jia, D. T. Cao, and Y. P. Liang, "Impermeability evaluation method and its application on the ancient weathering crust of carbonatite in Middle Ordovician system in North China coalfield," *Journal of China Coal Society*, vol. 39, no. 8, pp. 1735–1741, 2014.

[6] X. Y. Wang, M. J. Yao, J. G. Zhang et al., "Evaluation of water bursting in coal seam floor based on improved AHP and fuzzy variable set theory," *Journal of Mining and Safety Engineering*, vol. 36, no. 3, pp. 558–565, 2019.

[7] P. S. Zhang, W. Yan, W. Q. Zhang, Y. W. Yang, and Y. F. An, "Study on factors influencing groundwater inrush induced by backstopping of a coal seam with a hidden fault," *Journal of Mining and Safety Engineering*, vol. 35, no. 4, pp. 765–772, 2018.

[8] J. Sun, L. G. Wang, and H. F. Lu, "The analysis of the water-inrush dangerous areas in the inclined coal seam floor based on the theory of water-resisting key strata," *Journal of Mining and Safety Engineering*, vol. 37, no. 4, pp. 655–662, 2017.

[9] L. M. Yin, W. J. Guo, and C. Lu, "Patterns of the water-inrush hazard in the floor strata in deep mines and its catastrophic characteristics," *Journal of Mining and Safety Engineering*, vol. 34, no. 3, pp. 459–463, 2017.

[10] B. Li and Q. Wu, "An analysis of parameters sensitivity for vulnerability assessment of groundwater inrush during mining from underlying aquifers based on variable weight model," *Journal of Mining and Safety Engineering*, vol. 32, no. 6, pp. 911–917, 2015.

[11] L. Q. Shi, X. Y. Qu, J. Han et al., "Multi-model fusion for assessing the risk of inrush of limestone karst water through mine floor," *Journal of China Coal Society*, vol. 44, no. 8, pp. 2484–2493, 2019.

[12] L. Q. Shi, X. P. Tan, J. Wang, X. K. Ji, C. Niu, and D. J. Xu, "Risk assessment of water inrush based on PCA-Fuzzy-PSO-SVC," *Journal of China Coal Society*, vol. 40, no. 1, pp. 167–171, 2015.

[13] W. Q. Zhang, K. Zhao, G. B. Zhang, and Y. Dong, "Prediction of floor failure depth based on grey correlation analysis theory," *Journal of China Coal Society*, vol. 40, no. S1, pp. 53–59, 2015.

[14] W. Q. Zhang, G. P. Zhang, W. Li, and X. Hua, "A model of Fisher's discriminant analysis for evaluating water inrush risk from coal seam floor," *Journal of China Coal Society*, vol. 38, no. 10, pp. 1831–1836, 2013.

[15] Q. Wu, Z. L. Zhang, and J. F. Ma, "A new practical methodology of the coal floor water bursting evaluating: the master controlling index system construction," *Journal of China Coal Society*, vol. 32, no. 1, pp. 42–47, 2007.

[16] Q. Wu, Z. L. Zhang, S. Y. Zhang, and J. F. Ma, "A new practical methodology of the coal floor water bursting evaluating: the vulnerable index method," *Journal of China Coal Society*, vol. 32, no. 11, pp. 1121–1126, 2007.

[17] Q. Wu, S. H. Xie, Z. J. Pei, and J. F. Ma, "A new practical methodology of the coal floor water bursting evaluating: the application of ANN vulnerable index method based on GIS," *Journal of China Coal Society*, vol. 32, no. 12, pp. 1301–1306, 2007.

[18] Q. Wu, J. H. Wang, D. H. Liu, F. P. Cui, and S. Q. Liu, "A new practical methodology of the coal floor water bursting evaluating: the application of AHP vulnerable index method based on GIS," *Journal of China Coal Society*, vol. 34, no. 2, pp. 233–238, 2009.

[19] Q. Wu, B. Zhang, W. D. Zhao, and S. Q. Liu, "A new practical methodology of coal seam floor water burst evaluation: the comparison study among ANN, the weight of evidence and the logistic regression vulnerable index method based on GIS," *Journal of China Coal Society*, vol. 38, no. 3, pp. 21–26, 2013.

[20] B. N. Hu, H. X. Zhang, and G. B. Shen, *Guidebook of Setting Pillar and Pressure Mining under Buildings, Water Bodies, Railways and Development Roadway*, Coal Industry Publishing House, Beijing, China, 2017.

[21] L. Q. Shi, D. J. Xu, and M. Qiu, "Improved on the formula about the depth of damaged floor in working area," *Journal of China Coal Society*, vol. 38, no. S2, pp. 299–303, 2013.

[22] Y. C. Xu and Y. Yang, "Applicability analysis on statistical formula for failure depth of coal seam floor in deep mine," *Coal Science Technology*, vol. 41, no. 9, pp. 129–132, 2013.

[23] X. G. Yu, *Study on Broken Depth of Mining Damage Floor*, Shandong University of Science and Technology, Qingdao, China, 2011.

[24] X. G. Yu, L. Q. Shi, and J. Han, *Fractal Forecast Theory and its Application of Broken Depth of Damage Floor*, Coal Industry Publishing House, Beijing, China, 2016.

[25] L. Q. Shi, J. C. Wei, X. G. Yu, J. Han, L. Zhu, and P. H. Zhao, *Forecast of Floor Water Bursting Based on Information Fusion*, China University of Mining and Technology Press, Xuzhou, China, 2009.

[26] S. N. Dong, H. Wang, and W. Z. Zhang, "Judgment criteria with utilization and grouting reconstruction of top Ordovician limestone and floor damage depth in North China coal field," *Journal of China Coal Society*, vol. 44, no. 7, pp. 2216–2226, 2019.

[27] Y. Zhao, Y. Wang, W. Wang, L. Tang, Q. Liu, and G. Cheng, "Modeling of rheological fracture behavior of rock cracks subjected to hydraulic pressure and far field stresses," *Theoretical and Applied Fracture Mechanics*, vol. 101, pp. 59–66, 2019.

[28] J. Feng, S. J. Wang, and S. L. Deng, "Influence and protection of confined water resources by coal seam mining in Weibei coal mining area," *Journal of China Coal Society*, vol. 43, no. S1, pp. 269–276, 2018.

[29] Y. L. Zhao, L. Y. Zhang, J. Liao, W. J. Wang, Q. Liu, and L. Tang, "Experimental study of fracture toughness and subcritical crack growth of three rocks under different environments," *International Journal of Geomechanics*, vol. 20, no. 8, Article ID 04020128, 2018.

[30] J. Sun, L. G. Wang, and Y. Hu, "Mechanical criteria and sensitivity analysis of water inrush through a mining fault above confined aquifers," *Arabian Journal of Geosciences*, vol. 12, no. 4, p. 12, 2019.

[31] Y. L. Zhao, L. Y. Zhang, W. J. Wang, Q. Liu, L. M. Tang, and G. Cheng, "Experimental study on shear behavior and a revised shear strength model for infilled rock joints," *International Journal of Geomechanics*, vol. 20, no. 9, Article ID 04020141, 2020.

[32] J. Sun, L. G. Wang, and G. Zhao, "Failure characteristics and confined permeability of an inclined coal seam floor in fluid-solid coupling," *Advances in Civil Engineering*, vol. 2018, Article ID 2356390, 12 pages, 2018.

[33] Y. Zhao, C. Zhang, Y. Wang, and H. Lin, "Shear-related roughness classification and strength model of natural rock joint based on fuzzy comprehensive evaluation," *International Journal of Rock Mechanics and Mining Sciences*, vol. 137, Article ID 104550, 2021.

[34] D. Jin, G. Zheng, Z. Liu, and B. Chen, "Real-time monitoring and early warning of water inrush in a coal seam floor: a case study," *Mine Water and the Environment*, vol. 40, no. 2, pp. 378–388, 2021.

[35] B. Jiang, B. Ren, M. Su et al., "A new quantitative method for risk assessment of coal floor water inrush based on PSR theory and extension cloud model," *Geofluids*, vol. 2021, Article ID 5520351, 9 pages, 2021.

[36] L. Xiao, Q. Wu, C. Niu et al., "Application of a new evaluation method for floor water inrush risk from the Ordovician fissure confined aquifer in Xiayukou coal mine, Shanxi, China," *Carbonates and Evaporites*, vol. 35, no. 3, 2020.

[37] M. G. Qian, P. W. Shi, and J. l. Xu, *Mining Pressure and Strata Control*, China University of Mining and Technology Press, Xuzhou, China, 2010.

[38] J. l. Xu, *Evolution Law and Application of Mining Induced Fractures in Strata*, China University of Mining and Technology Press, Xuzhou, China, 2016.

[39] L. Yuan and S. S. Peng, *Proceedings of 36th International Conferences on Ground Control in Mining (China 2017)*, China University of Mining and Technology Press, Xuzhou, China, 2017.

[40] F. X. Jiang, *Mining Pressure and Strata Control*, China Coal Industry Publishing House, Beijing, China, 2004.